LUND
UNIVERSITY

Water assisted CO intercalation underneath Ir(111) supported graphene studied with scanning tunneling microscopy

Author:
Kaivalyakumar Mevada

Supervisors:
Jan Knudsen

Foteini Ravani

Master Thesis
VT 2016
Div. of Synchrotron
Radiation Research

January 10, 2017

Abstract

Graphene have attracted attention recently due to its unique properties and opportunities for development of high performance carbon based devices. The intercalation, absorption and reactions processes of small molecules above and below the graphene islands hold the key for new perspectives in catalysis, molecular sensors and other technologies. The present master thesis is focused on the investigation of the process for the intercalation of small molecules, such as Carbon Monoxide (CO), below graphene islands under Ultra High Vacuum conditions using Scanning Tunneling Microscopy (STM). It has been proven that the intercalation is facilitated with the presence of water under graphene islands. The water is formed underneath graphene by sequentially dosing of oxygen and hydrogen molecules. The formed water is visible with STM and preferentially located in the graphene edges and across the graphene islands grown on Ir(111) step edges. This phase raised the height of graphene by approximately 100 pm leading the graphene areas to be elevated from the Ir substrate. Furthermore, different amount of CO were dosed and STM was used to study the intercalation process. On saturating the surface with CO, digital CO intercalation was achieved below water phased graphene islands at room temperature and low pressures (in the range of 10^{-5}mbar). Digital intercalation means graphene areas where fully intercalated by CO molecules or not at all. The graphene corrugation (ripples) was also decreased by one order of magnitude, as compared to pristine graphene. Finally the intercalation at 1×10^{-8} mbar CO exposure was also studied using STM. Irregular shaped CO channels were formed under graphene islands crossing over Ir(111) step edge suggested a possible mechanism for the CO intercalation. The STM studies gained from this intercalation method and the proposed edge mechanism can give an insight on the design of new graphene interfaces.

Acknowledgements

Foremost, I would like to give special thanks to my supervisors, Jan Knudsen and Foteini Ravani for the guidance, discussion and encouragement they have given me throughout the work. Without their support, this thesis would not exist. I also wish to thank Alif Arman, Anders Mikkelsen, Estephania Lira, for helping me in the laboratory. I would also like to thank Jonathan Peterson for his company in lab and in writing our thesis.

Contents

Acronym Page

CNT	Carbon nano-tube
UHV	Ultra high vacuum
STM	Scanning tunnelling microscope
FCC	Face centered cubic
HCP	Hexagonal closed pack
TPG	Temperature programmed growth
CVD	Chemical vapor deposition
RT	Room temperature
ML	Mono-layer
LDOS	Local density of states
LEED	Low energy electron diffraction
L (unit)	Langmuir (1.33×10^{-6} mbar × 1 second)

Introduction

The field of nanoscience has grown rapidly over the past thirty years. One reasons for this is that materials often change properties dramatically when their sizes are changed to the nano-scale length scale. These unique properties of nano-scaled materials can be utilized to improve existing products.

In electronics, applications of nano-carbon materials have the potential to make superior electronic devices but much more research and development is needed before industrial production of devices in large quantities can be achieved [1, 2]. Nano-carbon materials can also be utilized both as membranes that traps reactants and products and as support materials for catalyst materials [3, 4].

Carbon has the ability to form structures with different structures. These different structures are often named allotropes, and figure 1 shows different such allotropes: Diamond structure (figure 1a.), Graphite (figure 1b.), A graphene sheet (figure 3c.), Carbon nano-tube (CNT) (figure 1d.), and fullerene (figure 1e.) [5].

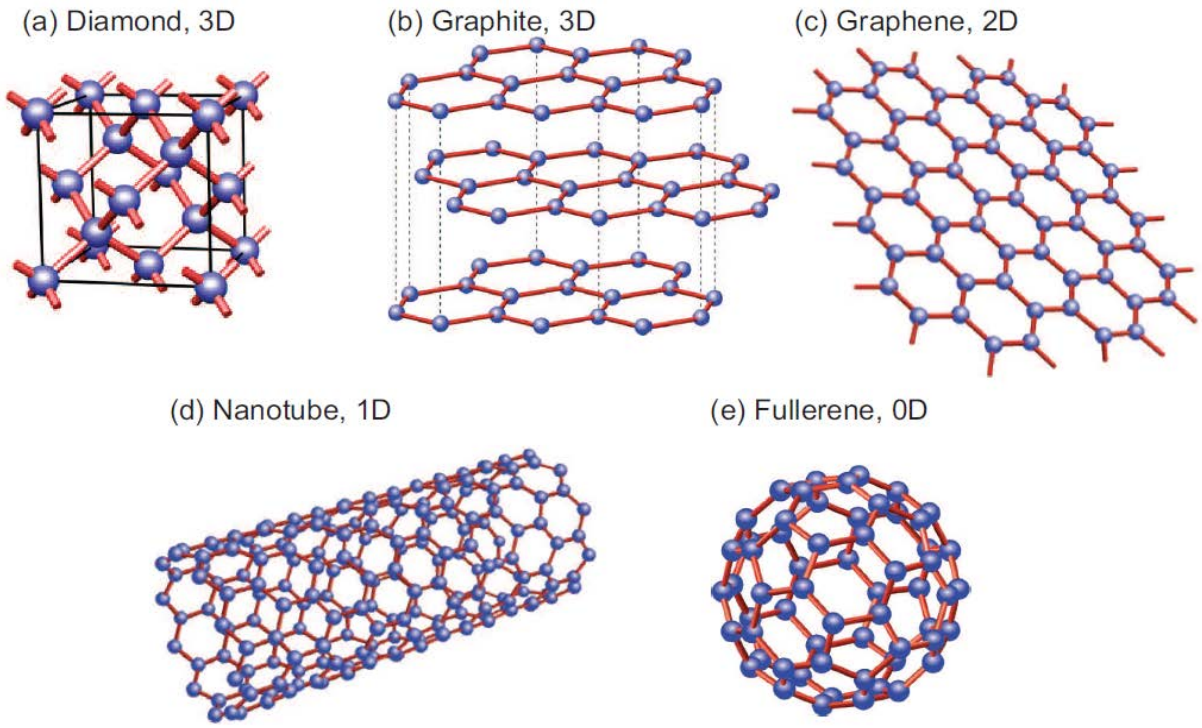

Figure 1: Carbon allotropes: (a) diamond, (b) graphite, (c) graphene, (d) carbon nanotube, and (e) fullerene. Figure taken from ref. [6]

These carbon structures exhibit different properties. For example, diamond is considered one of the hardest materials in comparison with graphite which is brittle and slippery. Furthermore, diamond is an electrical insulator while graphite is a good conductor.

Graphene can be described as a single layer of graphite. It was discovered in 2004 by Konstantin Novoselov and Andre Geim (University of Manchester) and they were awarded the Nobel Prize in Physics 2010 for their discovery. The unique properties that make graphene an intensive research material are the very high tensile strength, stiffness, low density, high electron mobility, and high opacity [7, 8, 9, 10]. Carbon nano-tubes (CNT) can be considered as a cylindrical grapheme sheet. Therefore, graphene can be considered as a mother material of CNT and graphite. Fullerene is a combination of pentagon and hexagon rings with carbon atoms at each vertex.

Graphene growth on different substrates exhibits different properties which can also be tuned through molecular interactions. Nowadays even the adsorption of a single molecule on graphene can be detected. Therefore, graphene has huge potential in gas-sensing devices [11].Furthermore, molecular intercalation of graphene can be used to detach graphene from its substrate and transfer it to another one [12, 13]. Here, the term intercalation refers to the process where atoms

or molecules diffuse in-between graphene and its substrate as illustrated in figure 2. Intercalation of atoms or molecules are, however, also interesting from a catalytic point as the graphene layer together with the substrate forms a nano-sized reactor, which can be used to study confined chemistry underneath graphene [14, 15].

Previous intercalation studies of graphene sheets shows that molecules can be successfully trapped below graphene upon gas dosing both at ultra-high vacuum and high pressure conditions [16]. In this project I used scanning tunneling microscopy (STM) to study how water islands trapped between graphene islands and the Ir(111) substrate can be used to facilitate carbon monoxide (CO) intercalation at low pressure. Water islands elevate graphene islands from the Ir substrate creating small gaps, this gap helps in diffusion of CO under graphene. I found that CO channels first are formed at Ir(111) step edges under the water intercalated graphene islands. From these CO channels the CO spread inwards into irregular shaped structures below the graphene islands at low CO exposures. On the other hand at high CO exposure leads to digital intercalation i.e. graphene islands are either fully intercalated or not at all. Finally in my thesis, a possible CO intercalation mechanism is also proposed.

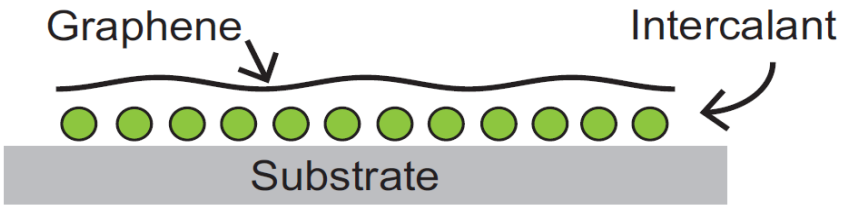

Figure 2: Illustration of graphene intercalation. The figure is taken from ref. [6]

Chapter 1 Background

1.1 Ir(111) surface

Iridium (Ir) is a transition metal of the platinum group with melting point above 2700 K. It is corrosion resistant, even at temperature as high as 2300 K [17]. Ir has an FCC (Face Centered Cubic) crystal structure as shown in the figure 3. The, Ir(111) surface is shaded red in figure 3. The unit cell of Ir(111) surface is hexagonal with nearest neighbor distance of 2.715 Å [6].

Generally, high quality graphene layers can be grown on various metal substrates. According to the literature transition metals like Rh, Ru, Ir, and Pt are excellent substrates for graphene growth [18, 19]. On Ir(111) it is possible to grow perfect graphene islands extending over several μm in contrast to other transition metals [20]. For that reason the Ir(111) surface was used as substrate in the current project.

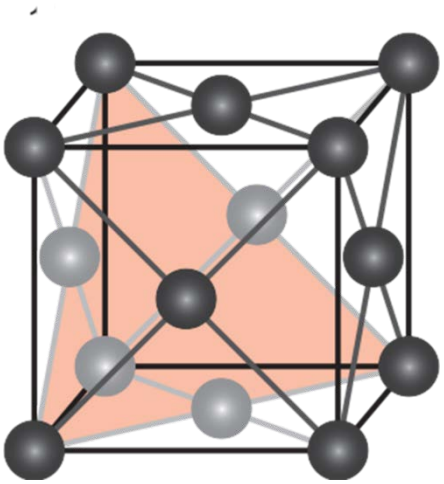

Figure 3: FCC unit cell, with the (111) plane shaded in red. The figure is taken from ref. [6]

1.2 Structure of Graphene on Ir(111) surface

A sketch of free standing graphene is shown in figure 4. This structure is also known as a honeycomb structure. The unit cell is marked with red parallelogram having side lengths of 2.46 Å.

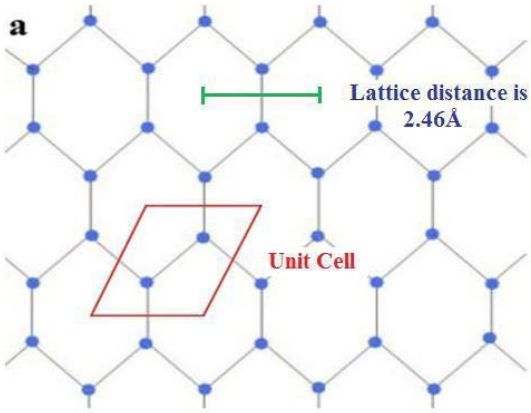

Figure 4: Structure of free standing graphene. The figure is taken from ref. [16]

Figure 5 shows a ball model of graphene supported by Ir(111). The lattice distance of the carbon honeycomb structure of graphene and the hexagonal Ir(111) surface is 2.45 Å and 2.72 Å, respectively. Thus, it is apparent that they have a lattice mismatch of almost 10% giving rise to an incommensurate moiré superstructure [6]. In figure 5(a) the moiré superstructure is indicated with black dotted lines. The moiré superstructure has hexagonal symmetry with a moiré distance of 25.3 Å. The moiré unit cell contains approximately 200 carbon atoms and 86 Ir atoms (i.e. 10.32 × 10.32 carbon atoms to 9.32 × 9.32 Ir atoms) [21]. As seen in figure 5(a) the rotation of the unit cell of graphene is perfectly aligned with the unit cell of Ir substrate. Therefore, the moiré unit cell formed is also aligned with the Ir(111) unit cells. Within the moiré unit cell there are 3 high-symmetry regions. One region called TOP is where the center of the hexagon ring is located atop of an Ir atom with all the carbon atoms sitting in three fold hollow sites. The other two regions are the FCC and HCP (Hexagonal Closed Pack) where the position of carbon atoms alternates between being on top of Ir atom and sitting into the three fold hollow sites [6]. They can be distinguished by knowing the position of HCP and FCC regions of the Ir substrate. The graphene layer is not equidistant from the substrate. In the HCP regions the carbon atoms of graphene are stronger bound to the Ir(111) substrate and as a result the height of the graphene atoms is lower in these regions. In contrast, the carbon atoms bind weakly to the substrate in the TOP regions leading to a higher graphene height in these regions. The distance between TOP, HCP, and FCC regions and the Ir(111) surface is 3.71 Å, 3.27 Å and 3.29 Å, respectively, as shown in figure 5(c).

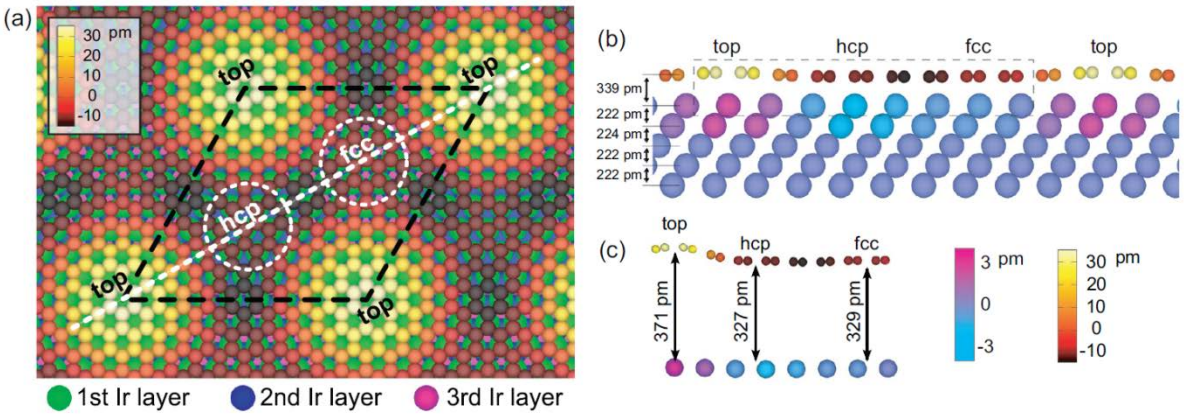

Figure 5: (a) Ball model of graphene grown on Ir(111) showing the carbon atoms in black-red-yellow color scale, and Ir surface, sub-surface, and sub-sub-surface with green, blue, and magenta color, respectively. Moiré unit cell is highlighted by black dashed line. (b) Cross-section along the diagonal of moiré unit cell marked by white dashed line in (a). (c) The dashed region in (b) is magnified to clearly show the buckling of graphene layer. The figure is taken from ref. [22].

Graphene is grown on Ir(111) substrate at high temperature (~1300 K). The thermal expansion coefficient of graphene is negligible as compared to that of Ir. It might be that the carbon atoms located at the graphene edges get strongly bonded to Ir surface atoms at high temperatures. Upon cooling the sample the Ir surface will shrink much more than the graphene islands and as a result they will get compressed. To release the stress wrinkles are often formed [23].

In graphene each carbon (C) atom bind to three adjacent C atoms, but at the edge C atoms have dangling bonds and they therefore form bonds with the Ir substrate atoms. As a result of the extra Ir-C bond formation at the edges the graphene edges bends downwards to the surface while the center of the islands is further away as shown in figure 6. Intercalation of graphene occurs in following manner, absorbates are first absorbed on the bare Ir(111) surface and from there they diffuse under graphene edges. Therefore, the way in which graphene is intercalated interacts with other atoms or molecules strongly depends on its edges. Hence, it is important to study small graphene islands [6].

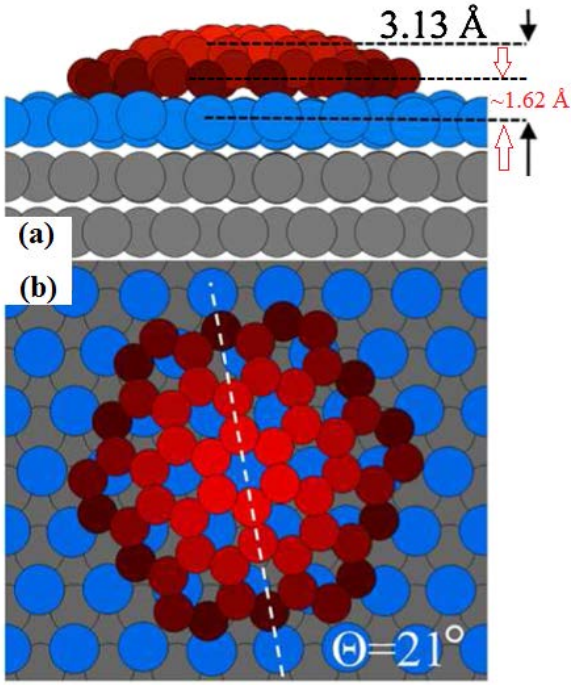

Figure 6: Ball model of graphene grown on Ir(111) showing the carbon atoms in red color scale. Carbon atoms closer to surface are dark red, while carbon atoms further away from the surface are light red. Ir(111) surface atoms are colored with blue, while substrate atoms are shown in grey. (a) Side view of graphene island on Ir(111). (b) Top view of graphene island on Ir(111). Figure is taken from ref. [24].

Chapter 2 Experimental methods

In this chapter the techniques and methods used in this thesis are discussed. The chapter begins with the description of temperature programmed growth (TPG) and chemical vapor deposition (CVD) grown graphene. Finally, the principles of scanning tunneling microscopy (STM) are discussed.

2.1 Temperature programmed growth (TPG)

In the TPG processes the metal surface acts as catalyst for dissociation of a carbon hydride such as ethylene or propene (C_2H_4, C_3H_6). The hydrocarbons are first absorbed on the metal surface at room temperature (RT) and subsequently annealed to high temperature in UHV [6]. In this master thesis ethylene was used as a carbon source while the sample was annealed to approximately 1300 K. The Ir(111) crystal was mounted on a molybdenum sample holder whose melting point is approximately 2900 K.

Regarding the mechanism, the absorbed C_2H_4 molecules on the Ir(111) surface decomposed above 820 K on Ir(111) [25, 26]. Hydrogen desorbs from the surface leaving C-atoms on the surface. These atoms diffuse on the surface and merge together and form graphene islands, as shown in figure 7 [27, 28]. The higher the temperature, the higher the surface diffusion is. Hence, highly ordered and large islands of graphene are formed with increasing the annealing temperature.

Decomposition of a ethylene saturated Ir(111) surface therefore results into partial coverage of the Ir(111) surface by graphene. From previous studies it is known that one cycle of TPG gives approximately 20% of graphene coverage [27].

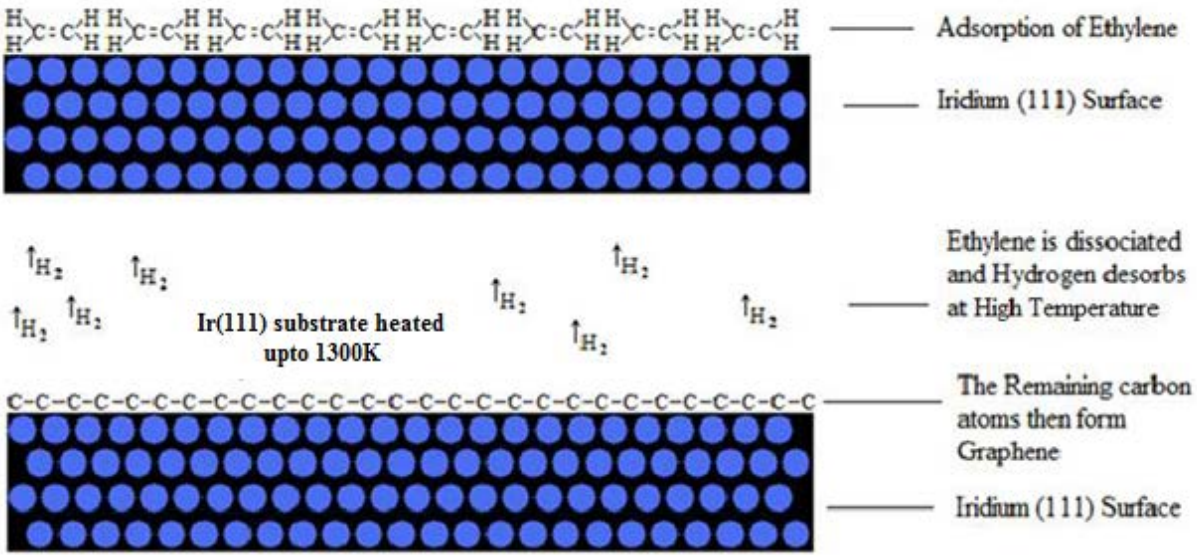

Figure 7: Illustration of the TPG process. Image taken from ref. [16]

After the first cycle of TPG there is 0.20×100 = 20% of graphene coverage. After the second cycle there is 20% + (0.20× (100-20)) = 36% and after third cycle there is 36% + (0.20 × (100-36)) = 48.8%. Thus, even by repeating this process for infinite number of times it will not result in 100% of graphene coverage, as each cycle only covers a fraction of the bare Ir surface. Furthermore, double layers of graphene are not formed, as the decomposition of carbon source occurs only on the bare metal surface.

The high quality of single layer graphene sheets and the control of the graphene coverage on metal substrates are some of the benefits of the TPG method. On the contrary, TPG is a time consuming method and cannot give 1 ML coverage.

2.2 Chemical Vapor Deposition (CVD)

In the CVD process, contrary to TPG process, the hydrocarbon molecules are dosed directly onto a hot metal surface. Decomposition takes place immediately upon adsorption and then graphene islands are formed from the C atoms formed from the dissociation, as shown in figure 8.The orientation of graphene islands formed by CVD process depends strongly on the temperature of the hot metal surface [27, 29]. The coverage of graphene can be tuned by controlling the dose of hydrocarbon molecules and by dosing large amounts of hydrocarbons full coverage of graphene over Ir(111) surface can be achieved.

Graphene growth at temperatures below 1000 K shows varieties of orientation, while graphene growth at temperatures above 1300 K has one single orientation. Graphene with different orientation exhibits different physical properties and moiré lattice distance but the graphene lattice distance remains constant [28, 30].

However, CVD cannot be done at high temperatures (>1400 K) due to the low sticking coefficient of the ethylene (hydrocarbon) to the metal surface. Moreover, another layer is not formed on graphene as ethylene is not adsorbed on graphene because the sticking coefficient of ethylene on graphene is nearly zero at such high growth temperatures [31].

To summarize, many different orientations of graphene can be achieved by using the CVD method to grow graphene on metal surfaces. Additionally, CVD does not give good control over graphene coverage.

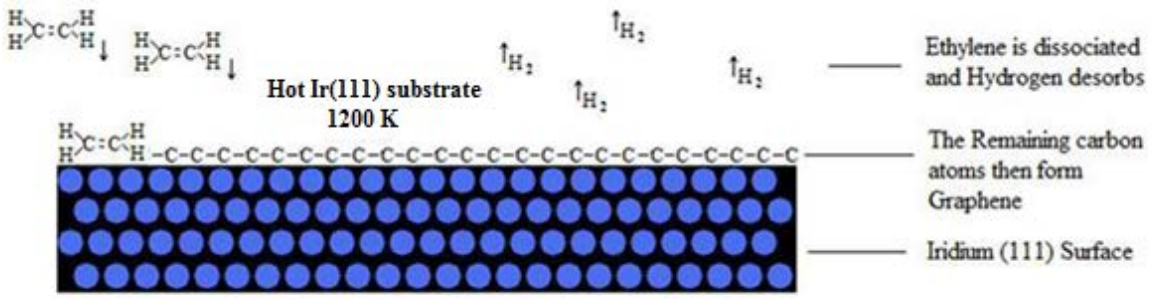

Figure 8: Illustration of the CVD process. Figure taken from ref. [16]

2.3 TPG + CVD

Graphene can also be grown using combinations of the CVD and TPG process. Initially, one cycle of TPG is used to produce graphene islands with single orientation as shown in figure 9(a-b). After that CVD is used to grow more graphene islands. The graphene grown by CVD will follow the orientation of graphene already grown by TPG, as shown in figure 9(c). When ethylene is dosed for extended period of time full coverage of graphene can be obtained as shown in figure 9(d). Thus, we have more graphene with one single orientation. This method can also be used as a fast way to produce large graphene islands.

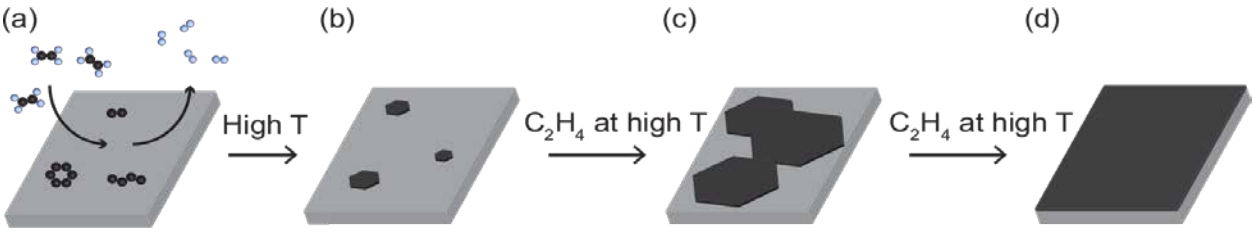

Figure 9: Illustration of the TPG + CVD process. The figure is taken from ref. [6]

2.4 Scanning Tunneling Microscopy (STM)

Scanning Tunneling Microscopy (STM) was developed in the early 80s by Gerd Binnig and Heinrich Rohrer (two physicists at IBM research division in Zurich) who shared the Nobel Prize in 1986 [32]. It is widely used in fundamental research in order to image and manipulate atoms, particles, and small molecules. It is a novel technique that yields surface topographies in real space, and it can be used to image surface defects [6].

2.4.1 Working principle

STM gives direct real space images of surface structures and with settings and a beneficial tip structure it is possible to obtain atomic resolution. The spatial resolution is approximately 1 Å in the surface plane and 0.1 Å in perpendicular direction [33]. In addition to the real space imaging of surfaces, the STM can also be used to manipulate single atoms or molecules on surfaces.

STM is based on the quantum mechanical tunneling of electrons through a vacuum barrier. When the tip is in close vicinity of a surface and a bias voltage is applied between the tip and the surface, electrons starts to tunnel through the vacuum barrier formed by tip and surface work functions. This generates a tunnel current and it is highly sensitive to the distance between tip and surface. The measured tunneling current is used to create the images of the surface.

2.4.2 Tunneling effect in STM

To understand the concept of tunneling in STM, a simplified 1D system of two conducting materials (tip and sample) separated by a potential barrier (vacuum) can be considered. Figure 10(a) shows the wave function in the tip, vacuum, and sample. The wave function of tip leaks out exponentially in vacuum with an inverse decay length K given by

$$K = \frac{\sqrt{2m\Phi}}{\hbar} \tag{1}$$

Where, m is the electron, Φ is average work function of the tip and the sample, and ħ is Plank's constant [34].

Without a bias voltage applied there is no net flow of electrons between the tip and the sample. But, when a bias voltage is applied there is a net flow of electrons from filled states of the sample/tip to empty states in tip/sample. Figure 10(b) shows the shift in Fermi level of sample and tip, when the sample is positively biased and the net flow of electrons from the filled states of tip into the empty states of the sample. When the sample is negatively biased the net flow of electron will be from the filled states of sample into the empty states of tip. The current due to this net flow of electron is called tunneling current. A simple equation of tunneling current can be given by [2, 34]

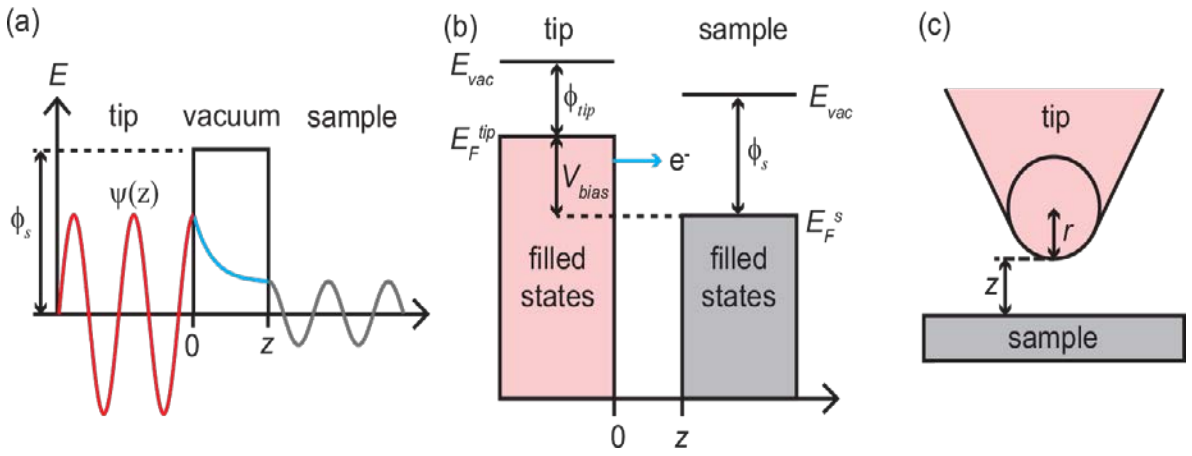

Figure 10: (a) The wave function in tip, vacuum, and sample. (b) Fermi levels of tip and sample with positive biased applied to sample. (c) Atomically sharp tip over sample. Figure taken from ref. [6]

$$I \propto V_{bias} \rho_s \rho_t e^{-Kd} \tag{2}$$

Here, V_{bias} is bias voltage applied between sample and tip, ρ_s and ρ_t are the local density of states (LDOS) of sample and tip, d is the distance between the tip and the sample, and K is given by equation (1). Figure 10(c) shows an atomically sharp tip over the sample and the distance (d) between the center of the atom and sample is Z + r. The number of electron states at certain energy at particular spatial location is given by LDOS. Tunneling current depends exponentially on the distance between the tip and sample as well as on the LDOS of tip and sample. Thus STM images are complex convolutions between the electronic structure and topography of sample surfaces and the apparent height is in general not equal to the absolute height of the surface.

2.4.3 Modes of operation

STM can be operated in two different scanning modes: constant height and constant current mode.

Constant height mode

While scanning in the constant height mode the tip is held at a constant height above the sample and the tunneling current is measured, as shown in figure 11(a). This measured value of tunneling current is used to generate the image.

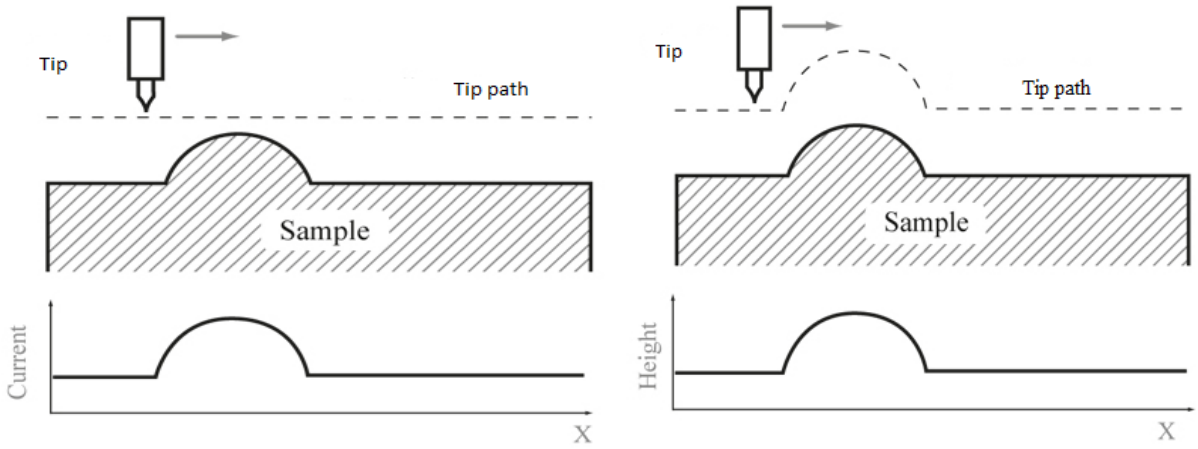

(a) (b)

Figure 11: (a) Illustration of constant height mode (b) Illustration of constant current mode. Figure taken from ref. [35]

Constant current mode

In constant current mode the tunnel current is kept constant and the change in tip height is measured as shown in figure 11(b). The current is kept constant at a fixed value, I_0, by using a feedback circuit. It will change the height of the tip when a change in current is detected. If the current decreases the tip is brought nearer to the sample until the current increased to I_0. Similarly, if the current increases the tip is retracted until the current decreases to I_0. Here the measured tip height is used to generate the image.

There are advantages and disadvantages of both the scanning methods. The constant height mode is faster as it measures directly without using the feedback circuit. However while scanning over a rough surface or a surface with several step as in this project, the tip can be destroyed by crashing into the surface. The constant current mode is slower due to the additional time required for the response of feedback circuit to adjust the tip position. Crashing of the tip is, however, prevented even if the surface is rough. Generally constant current mode gives better resolution than constant height mode. As the aim of this project was to study the surface structure and not any dynamic process, there was no need to scan fast. All the STM images in this thesis are obtained by scanning in constant current mode. Typically the time required to acquire a STM image is few minutes.

2.4.4 Set up of STM in the Obelix lab

An image and a schematic representation of the scanning tunneling microscope I used for my studies are shown in figure 12 and 13, respectively. The main components of the STM unit are a sharp metal tip, piezo electric elements, and a conducting sample. The three orthogonal piezo electric elements are attached to the scanning unit as shown in figure 12 and 13(a). The x and y piezo electric elements are used to raster scan the sample surface, while the z piezo controls the height of the tip from the sample surface [33]. The position of individual piezo electric element can be changed by applying appropriate voltage to them. This is done automatically by the software controlled voltage supplies. The sensitivity of piezoelectric element for expansion/contraction is approximately 1 Å/mV. This gives very accurate positioning of STM tip above the sample surface [33].

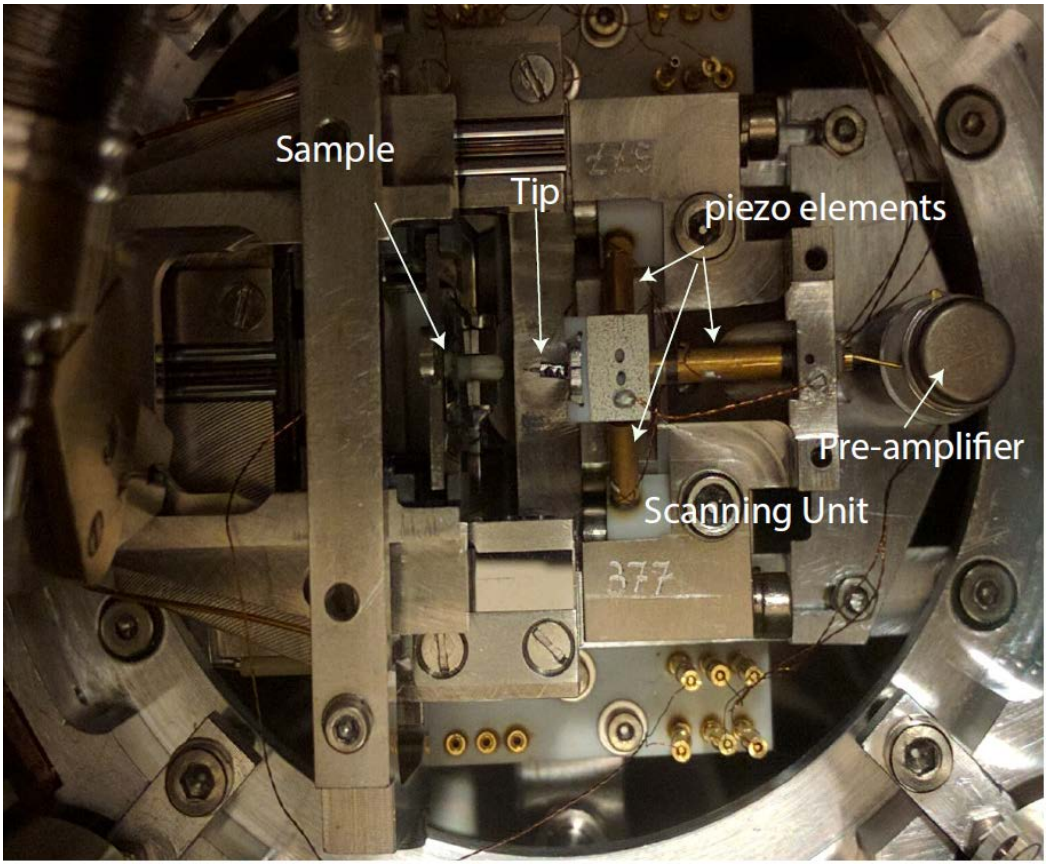

Figure 12: STM setup. Figure taken from ref. [36]

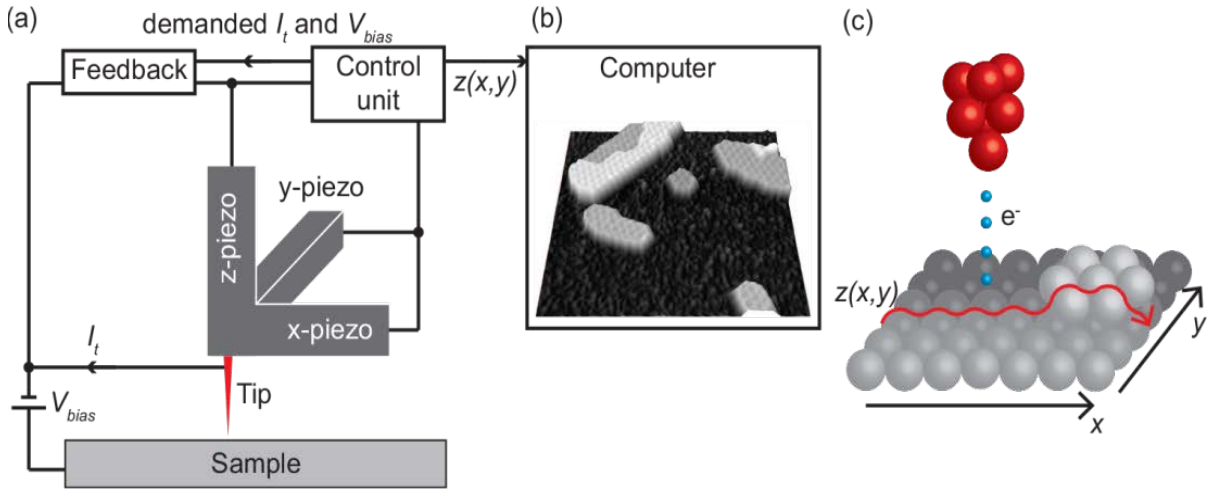

Figure 13: (a) Schematic representation of STM, (b) STM image generated in computer, (c) Magnified representation of tip scanning over the surface. Figure taken from ref. [6]

To get atomic resolution of the sample surface the tip needs to be atomically sharp as seen in figure 13(c). It is prepared through controlled chemical etching of thin tungsten wire. The tip is then mounted on the tip holder that can be mounted in the scanning unit. The sample is placed firmly in sample holder that will prevent vibrations during the scan. The sample holder can move in two dimensions: towards the tip and horizontally.

The sample is brought in close proximity of the tip for scanning, in following three steps. Initially the sample is fully back from the tip (~1cm) and the tip is retracted. By manually using camera and electronics, the sample is brought as close as possible to tip. Now the bias voltage and tunneling current are set to 1V and 1nA, respectively. An iterative approach is used: First, the sample moves one step forward towards the tip and then fully extending the tip to check if the specified tunneling current is achieved. If not the tip is retracted and the whole process is repeated until the required tunneling current is achieved. After that finer adjustment is done such that the Z piezo of tip is in the middle of its total moving range. To control the scanning parameters like the bias voltage, tunneling current, etc. software called MATRIX v3.2 was used.

The scanning tunneling microscope should be isolated from external vibration, arising from the surrounding environment, to avoid tip-sample collisions and distortions in the measured image. This can be done by isolating the scanning unit mechanically from the floor of the room with the help of springs or shock absorbing materials. Additionally, an eddy current damping system is also implemented for isolation from vibrations on the system I worked on. There are several ways to reshape the tip in situ and make it sharp again. One way is to apply voltage pulses to tip, so tip will reshape due to high electric field. Another way is to crash the tip into sample in controlled manner; this will also change the shape of tip.

2.4.5 Ultra-High Vacuum (UHV) system

The UHV system which was used during my master thesis is shown in figure 14. It is a versatile UHV system for preparation and characterization of monolayer and ultra-thin films. The system consists of two connected UHV chambers and one load lock chamber all isolated with valves.

The preparation chamber with a base pressure in the low 10^{-10} mbar regime is equipped with sputter gun, an electron beam heater which can heat the sample to ~ 1500 K, evaporators, gas lines, and a mass spectrometer. As the name indicates the preparation chamber is where the sample is prepared i.e. sample undergoes different procedures or treatments. To introduce the sample into the preparation chamber it is first placed in the holder of the load lock and the pressure is reduced up till 10^{-6} mbar. After that the sample is transferred into the preparation chamber. The sample temperature is measured with a type K thermocouple spot-welded to the edge of the crystal surface.

The sample can be transferred to the analysis chamber using a transfer arm. The analysis chamber has a base pressure in the 10^{-11}mbar range and is equipped with auger spectroscopy, low-energy electron diffraction LEED, and a STM stage. The analysis chamber also houses sample/tip storage carousel.

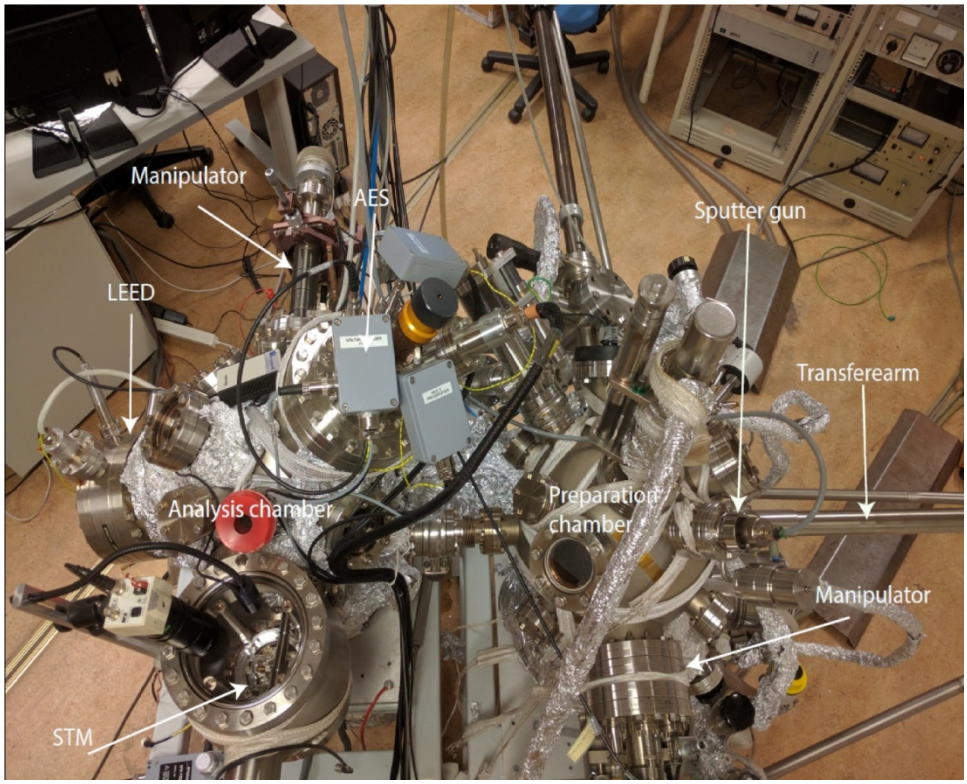

Figure 14: A photograph of UHV system in the lab. Figure taken from ref. [36]

Chapter 3 Results/Discussion

3.1 Clean Ir(111) surface

The Ir(111) surface was cleaned using number of cycles of Ar^+ sputtering at room temperature (1.5 keV energy, 15 min, 2.0×10^{-5} mbar pressure) with subsequent annealing to 1100 K – 1200 K in presence of O_2 (10 min, 5×10^{-7} mbar pressure) followed by flash annealing to 1400 K in vacuum.

Ar^+ sputtering is done to remove the surface layers of the Ir(111) single crystal surface. Annealing in presence of O_2 removes carbon contamination from the surface, while flashing removes absorbed oxygen from the surface as well as trapped Ar below the surface. If the flashing temperature is too low there might be some trapped Ar forming bubbles subsurface [6].

Figure 15 shows a characteristic STM image of the clean Ir(111) surface. The mono-atomic step edges and terraces are clearly visible. The length of terraces varies from 30 nm to 100 nm. Some Ar bubbles are also visible (white circled marked area).

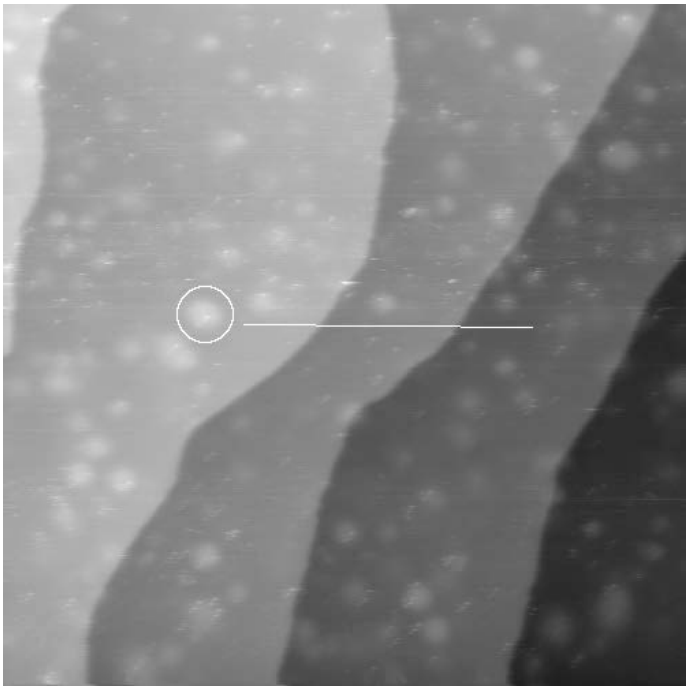

Figure 15: STM topography of clean Ir(111) surface (200×200 nm^2)

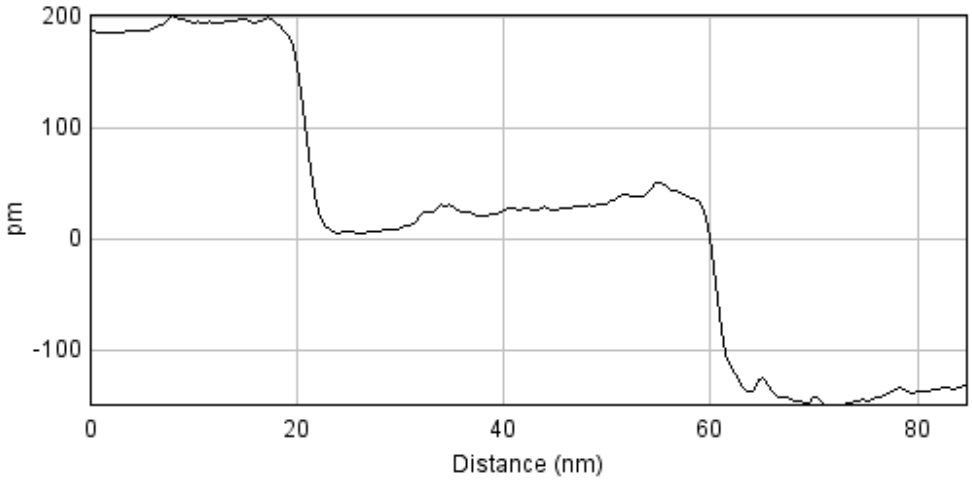

Figure 16: Line profile scan along the white line in figure 15.

The height of the steps on the Ir(111) surface was measured by STM. Figure 16 shows a height profile along the white line of figure 15.Two step edges are clearly visible in the line scan and the height of adjacent Ir(111) terraces is measured to be approximately 200 pm. The expected height difference is of 200 pm so there is almost 100 % accuracy in the obtained height profile.

3.2 Pristine graphene

First, graphene was grown using one cycle of TPG. C_2H_4 was dosed at room temperature for 100 seconds at 1×10^{-7} mbar pressure and subsequently annealed at 1300 K. This should result in approximately 0.2 ML of graphene coverage [6].

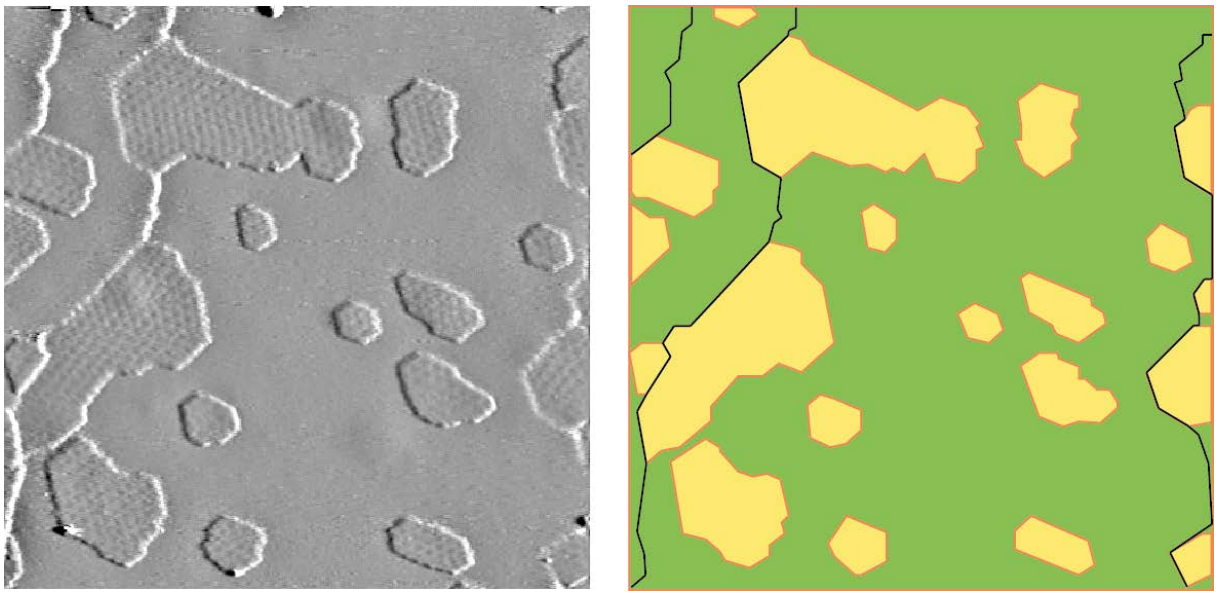

(a) (b)

Figure 17: (a) STM topography (100 × 100 nm) of graphene covering 24% Ir(111) surface. (b) Schematic of STM image where Ir(111) surface is represented in green, graphene in yellow and Ir step edges in black.

Graphene islands of different shapes and sizes with visible moiré pattern can be seen in figure 17(a). The calculated coverage of graphene islands on Ir(111) surface is 24%. A schematic representation of STM image is shown in figure 17(b), where the green and yellow regions denotes bare Ir(111) surface and graphene islands, respectively. Furthermore, the Ir step edges are represented by black lines. It can be inferred from the above images that larger graphene islands are formed on Ir(111) step edges while the smaller ones are located on the Ir(111) terraces. Furthermore, a larger portion of graphene islands crossing or attached to Ir steps, tends to be on the lower Ir(111) terrace.

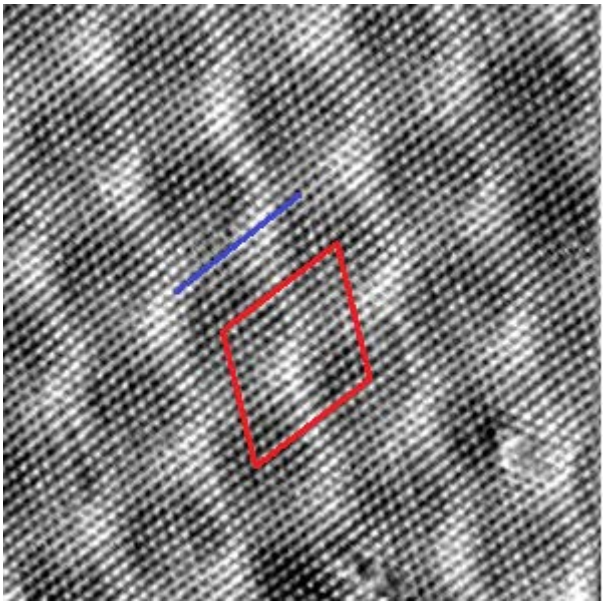

Figure 18: STM topography (10 × 10 nm) of graphene. The moiré unit cell is marked in red and the alignment of the carbon rings are marked in blue

Figure 18 shows a high resolution STM image of graphene. The moiré pattern and the carbon ring structure are clearly visible. The moiré unit cell is marked with a red parallelogram. It can be seen that moiré unit cell is aligned with the carbon rings (marked by blue line). The darker and the brighter regions represent the TOP and the HCP/FCC regions respectively as discussed above (see figure 5)

In all my experiments graphene was grown by a combination of TPG and CVD processes, as more graphene coverage was required. After one cycle of TPG at 1300 K the sample was cooled to 1200 K and ethylene was dosed for 60 second at 1×10^{-7} mbar pressure.

3.3 Water islands below graphene

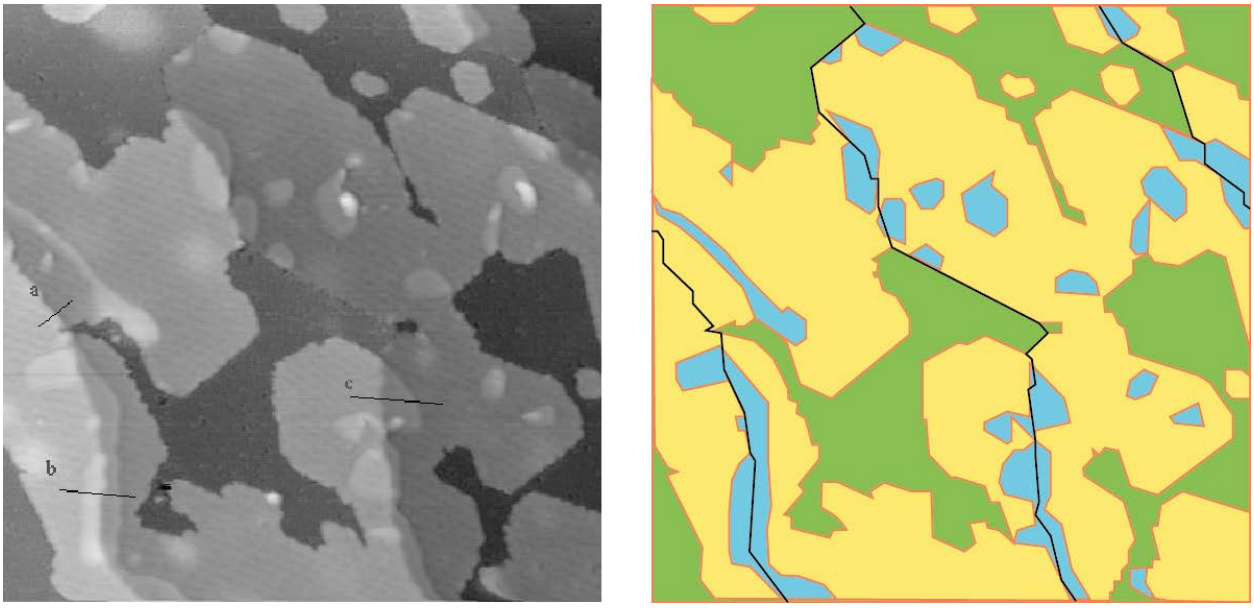

(a) (b)

Figure 19: (a) STM topography (100 × 100 nm) of graphene on Ir(111) surface after dosing 200 L of O_2 at 450 K and subsequently dosing 100 L of H_2 at room temperature . (b) Schematic of the STM image where water is represented by blue color.

After graphene growth the sample was exposed to 200L O_2 (200 seconds, 1×10^{-6} mbar pressure) at 450 K. Then the sample was cooled down to room temperature and (100L) H_2 was dosed for 100 seconds at 1×10^{-6} mbar pressure.

As established in E.Grånäset. al, ACS Nano6 , 9951 (2012) the oxygen molecules are absorbed on bare Ir(111) and dissociated to O-atoms [37]. At 450 K the oxygen atoms diffuse below the graphene islands where they form a p(2x1)-O structure [37]. During H_2 exposure, H_2 adsorbs on bare Ir(111) and dissociates to H-atoms. These H-atoms reacts with O-atoms on bare Ir to form water. But the sticking coefficient of water on bare Ir is negligible so it is instantly desorbed from the surface. H-atoms can, however, also diffuse under graphene and react with the O-atoms

to form water islands that here are trapped [37]. The structure of these water islands is known to be a super dense mixed OH/H_2O phase [6].

Figure 19(a) shows an STM image of graphene after dosing O_2 and H_2. The visible bright islands represent the water under graphene. Figure 19(b) is a schematic of the STM image where water is represented by blue color. Inspection of this figure reveals that graphene is partially intercalated by water and most of the water islands are located near Ir step edges. Further, it is found that the water below graphene is located away from the graphene edge for the graphene islands located on Ir terraces. Finally we find that there is no water under the small graphene islands lying on the terraces. This might be because on terrace the carbon atoms at the edge of graphene have to bend down to bond with Ir atoms which might create a barrier for intercalation [6], as shown in figure 20(a).

A statistical analysis of the STM images gives us the following results. The area coverage of graphene on Ir surface is on an average 36%, out of which the percentages of graphene islands attached, crossing over Ir step and on terrace are around 25%, 50% and 25%, respectively. This shows that graphene islands prefer to be crossing over Ir step edges.

The total area coverage of water under graphene islands is approximately 8 %. Furthermore, the percentages of water under graphene islands that are attached, crossing over Ir step and on terrace are around 7%, 65% and 28%, respectively.

Moreover, by doing an analysis of the length coverage of Ir step edges the following results were obtained. The length of Ir step edge attached by graphene islands was about 34% and crossed over by graphene was about 38%. The Ir step edges having water under graphene islands attached and crossing over were around 15% and 85%, respectively. This implies that almost all the graphene islands crossing over Ir step have water trapped beneath them. Thus it can be inferred that water prefers to sit in the gap formed when graphene islands are crossing over Ir step edges, as shown in figure 20(b).

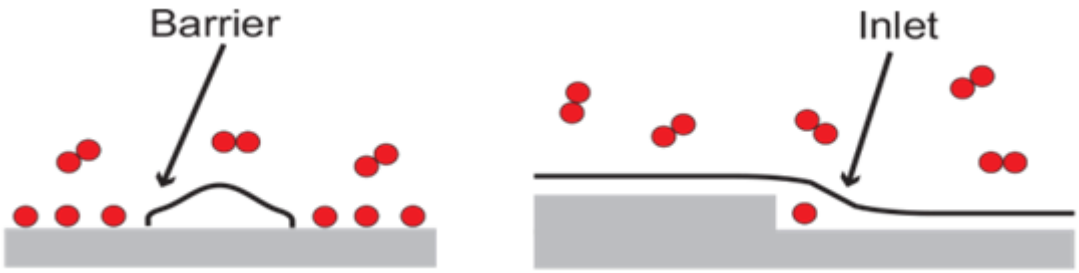

(a) (b)

Figure 20: (a) Illustration of how the gap at step edge facilitates intercalation, (b) Illustration of how the graphene edges hinder intercalation. The figure is taken from ref. [6]

Figure 21, 22, and 23 are the line scan done across the white line a, b, and c respectively, as shown in figure 19(a). The color codes used in here are same as the one used for schematic of STM images. Moreover, the terrace to the left of the Ir step edge (represented by black line) is always the upper terrace. The X-axis denotes the length for which the scan was done and Y-axis denotes height of the structure on surface. The absolute value of Y-axis is not important; it varies on the basis of how the raw STM image is edited in imageJ software. The difference in height of the structure is important.

Line profile analysis for the graphene crossing over Ir step reveals that the difference in height between the pristine graphene on upper terrace and lower terrace was approximately 200 pm, as shown in figure 21. Additionally, when graphene was intercalated by water only on the lower terrace, the graphene on the lower terrace was lifted up by approximately 100 pm, as shown in figure 22. Furthermore, when the graphene was intercalated by water on both the terraces, graphene on both terrace was lifted up by 100 pm, as shown in figure 23. But the difference in height of graphene on upper and lower terrace near the step edge was still around 200pm. So the gap formed when graphene island are crossing over Ir step edge should also increase by 100 pm. and may be this extra gap created might act as a channel for CO intercalation. There is no graphene island with full intercalation of water but from partial intercalation we know that water lifts graphene by 100 pm. Therefore, it can be concluded that height of water intercalated graphene should be 350 pm above Ir surface.

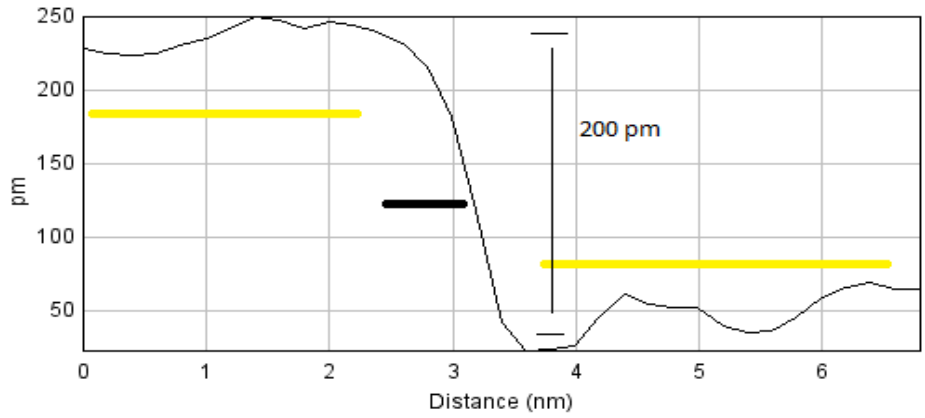

Figure 21: Line scan done across (pristine graphene) white line ‘a’ in figure 19(a).

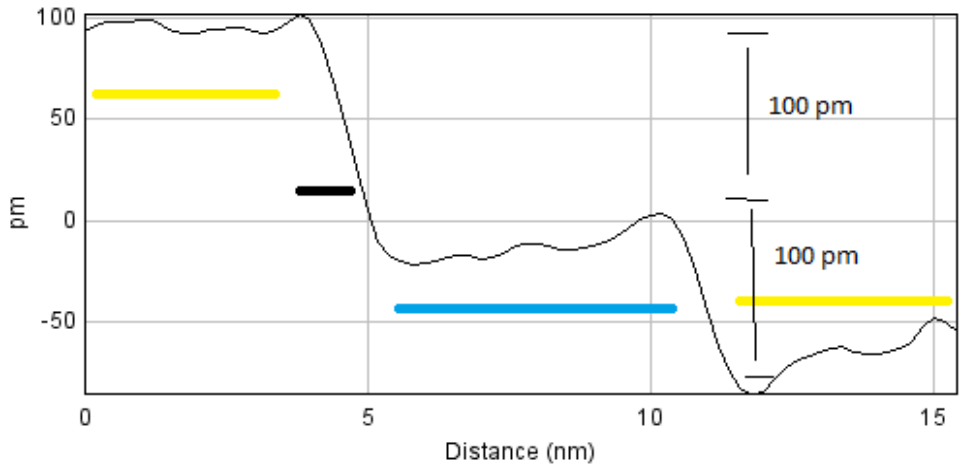

Figure 22: Line scan done across (water on lower terrace) white line ‘c’ in figure 19(a).

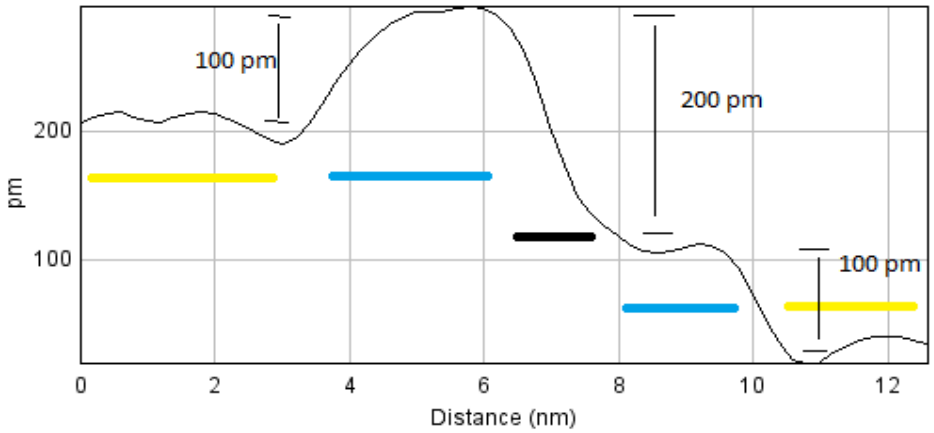

Figure 23: Line scan done across (water on both terraces) white line ‘b’ in figure 19(a).

3.4 Water assisted Carbon monoxide (CO) intercalation of graphene

3.4.1 CO (100L) dosed on water intercalated graphene

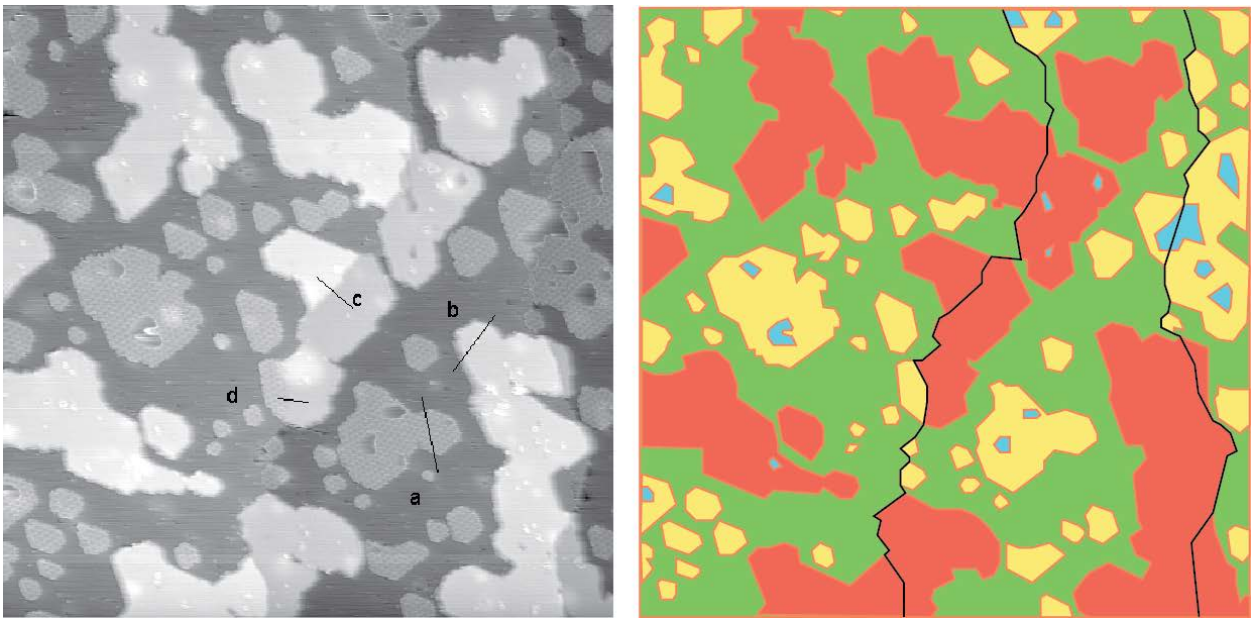

(a) (b)

Figure 24: (a) STM topogrphy (200 × 200 nm) of water intercalated graphene on Ir(111) surface after dosing 100 L of CO at room temperature. (b) Schematic of STM image where CO intercalated graphene is represented by orange color.

The water intercalated graphene was exposed to 100L of CO molecules for 100s at 1×10^{-6} mbar pressure at room temperature.

Figure 24(a) shows a STM image acquired after CO exposure and figure 24(b) is its schematic were CO intercalated graphene is shown by orange color. Pristine graphene, water intercalated graphene and CO intercalated graphene all are visible in this image. The relatively brighter graphene islands visible in figure 24(a) are the ones intercalated by CO molecules. There are no graphene islands, located on the same terrace, visible that are only partially intercalated by CO. All of them are either fully intercalated or not at all intercalated by CO and we therefore name this digital intercalation. Moreover, moiré pattern is not visible on CO intercalated graphene and the CO intercalated graphene islands edges appears to be smeared compared to the sharp edges

of non-CO intercalated graphene islands. This indicates the possibility of CO intercalated graphene islands' edges being detached from the Ir substrate.

Here the water appear to be black while in previous images of water intercalated graphene they were white. This is due to changes of the tip state. It can be inferred that almost all small graphene islands are not intercalated. There are some larger graphene islands on terrace that are intercalated by CO. All the graphene islands crossing over Ir step are intercalated except one. There is also a graphene island that is intercalated on lower terrace but not on upper terrace.

After the statistical analysis of STM images of graphene intercalated with CO following results were obtained. The relative area of graphene islands that were intercalated by CO was about 36%. Furthermore, the relative areas of CO intercalated graphene that was attached, crossing over Ir step and on terrace were approximately 30%, 60%, 28%, respectively. Thus the probability of intercalation by CO of graphene island crossing over Ir step is double than the other two. The percentage of water under the graphene that was not intercalated by CO was in range of 0% to 10% with an average of 5%.

If the small white spots visible on CO intercalated graphene are considered as water then the average percentage of water on CO intercalated graphene was 2%. Major proportion of water was at Ir step covered by graphene but only traces of it are visible at Ir step covered by CO intercalated graphene. So may be water under graphene is able to escape from graphene islands after CO intercalation.

From the analysis of the length coverage of Ir step edges following results are obtained. The average percentages of graphene attached and crossing over Ir step being intercalated by CO are 83% and 50%.

From the line profile analyses following results are obtained. Pristine graphene on terrace is approximately 250 pm above Ir surface, as shown in figure 25. While CO intercalated graphene on terrace is approximately 500 pm above Ir surface, as shown in figure 26. Thus after CO intercalation graphene is elevated by nearly 250 pm. Moreover the corrugation is decreased from 80 pm in pristine graphene to 10 pm in CO intercalated graphene.

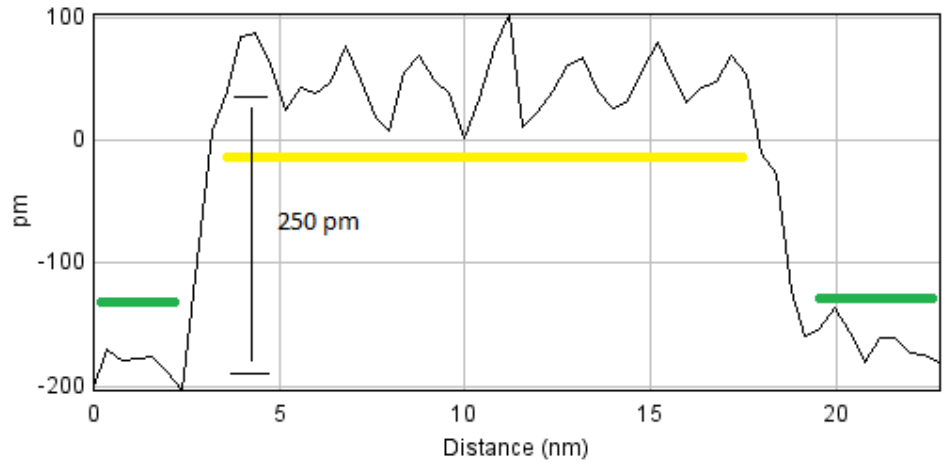

Figure 25: Line scan done across (pristine graphene on terrace) black line ‘a’ in figure 24(a).

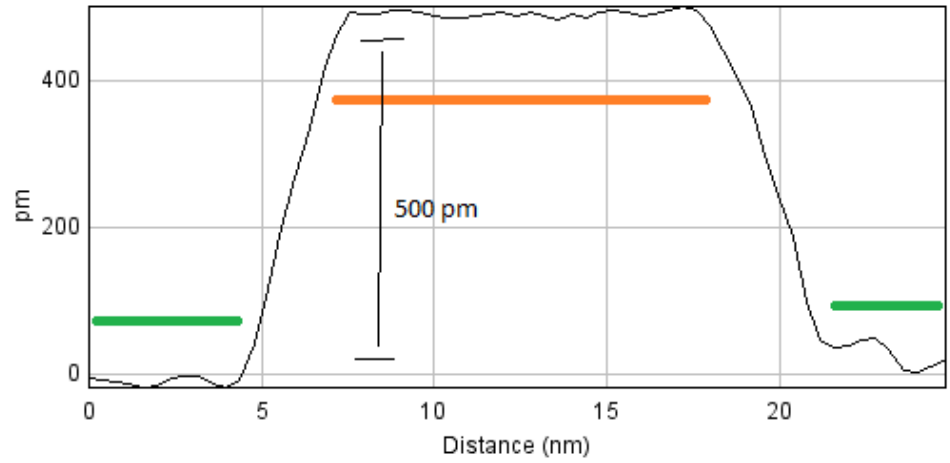

Figure 26: Line scan done across (CO on terrace) black line ‘b’ in figure 24(a).

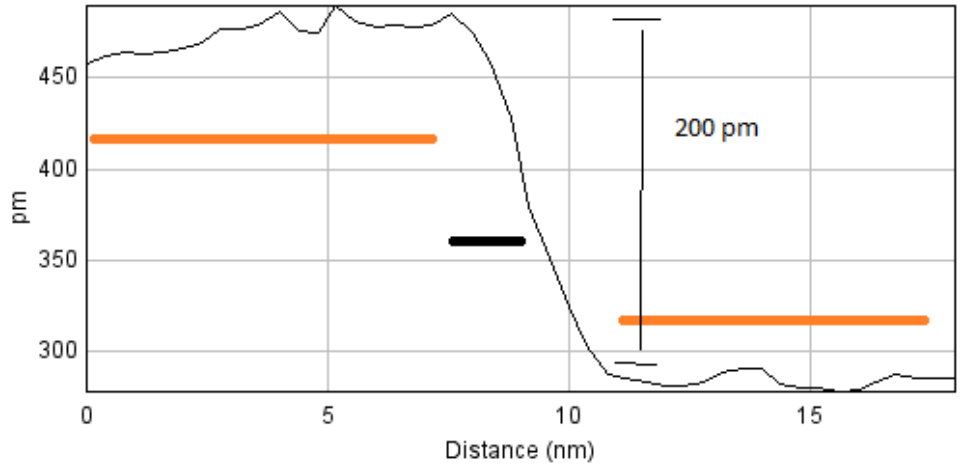

Figure 27: Line scan done across (CO on both terrace) black line ‘c’ in figure 24(a).

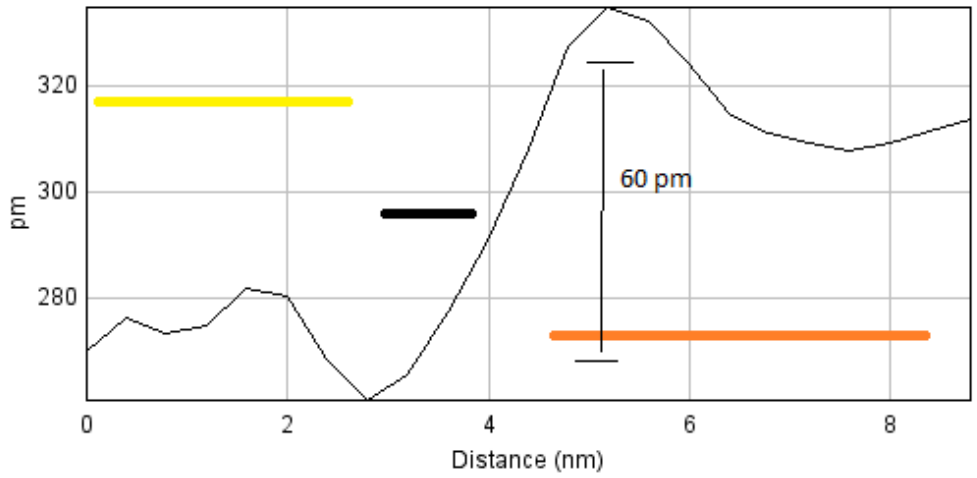

Figure 28: Line scan done across (CO on lower terrace) black line ‘d’ in figure 24(a).

The difference in height between fully CO intercalated graphene on upper terrace and lower terrace was approximately 200 pm, as shown in figure 27, which is same as observed in pristine graphene crossing over Ir step edge. Additionally, when graphene was intercalated by CO only on the lower terrace, the height of graphene on the lower terrace was approximately 60 pm above that height of graphene on upper terrace, as seen in figure 28. This also indicates the possibility of CO intercalated graphene being detached from Ir substrate.

3.4.2 CO (300L) dosed on H_2O intercalated graphene

After acquiring the STM images of the sample dosed with 100L of CO, more (200L) CO was dosed for 200 second at room temperature at 1×10^{-6} mbar pressure to check if more graphene islands become intercalated or the graphene islands already been saturated.

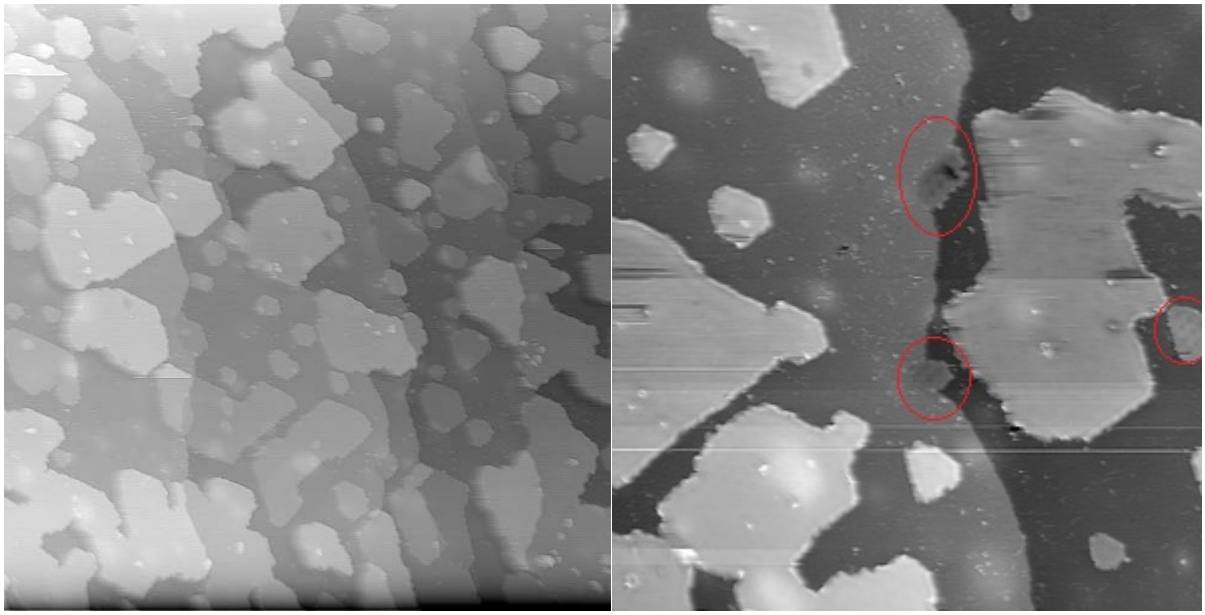

(a) (b)

Figure 29: Graphene structure after dosing 300L of CO. a) STM overview image (200 × 200 nm) b) STM image (100 × 100 nm) with non-intercalated islands are marked in red circles.

It can be inferred from figure 29(a) that the area coverage of CO intercalated graphene has increased. The average area coverage of CO intercalated graphene is above 81%. In figure 29(b) there are some small as well as big graphene islands are visible. All the big ones are CO intercalated. There are two types of small graphene islands visible, some are intercalated by CO and others are not intercalated.

It cannot be confirmed from the current information that the graphene islands that are intercalated by CO already had water underneath and the non-intercalated ones do not have water below them. There is also a possibility that the edges of graphene islands are modified during water formation, irrespective of graphene islands having water underneath or not, which enables CO intercalation.

3.4.3 CO (1L) and H_2O intercalated graphene

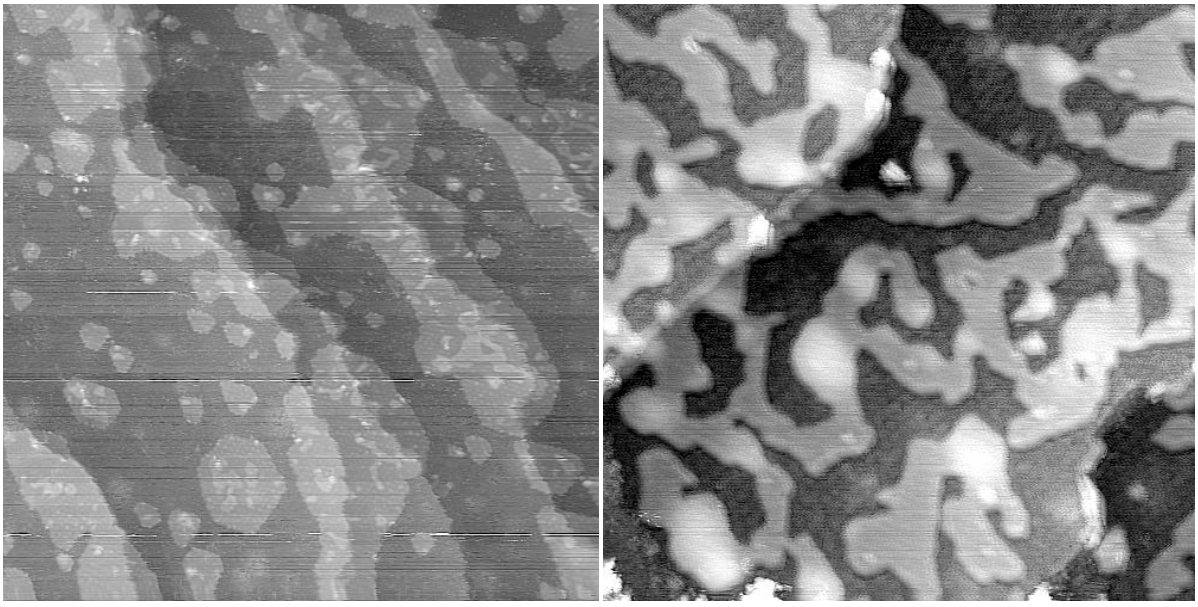

(a) (b)

Figure 30: Graphene structure after dosing 1L of CO (a) STM overview image (200 × 200 nm) that shows the starting of CO intercalation. (b) STM image (100 × 100 nm)

To study the initialization of CO intercalation very little amount (1L) of CO was dosed at room temperature for 100 seconds at 1×10^{-8} mbar pressure on to the water intercalated graphene.

Figure 30(a) shows a channel like structure formed under graphene islands, which are seen to be partially intercalated. These channels are visible on all type of graphene islands irrespective of whether they are found on terrace or crossing over the Ir steps. Figure 30(b) shows a zoom in STM image of a graphene island crossing over the Ir step. There is a thin channel formation along the Ir step edge and it is visible that all the channels on terrace are connected to channels at Ir step edges. Probably CO diffuses through these channels in under the graphene islands.

Conclusions

My project revealed that water intercalated graphene supported on Ir(111) facilitates CO intercalation even for low dosing pressure of 1×10^{-8} mbar. Firstly, water is formed underneath graphene by subsequently dosing O_2 and H_2 on the Ir(111) sample that was partially covered with graphene islands. A STM analysis revealed that most water is formed in the gap where graphene island cross over Ir step edges. Moreover, the graphene intercalated by water was raised by approximately 100 pm from Ir(111) surface.

Upon dosing (1L) CO at low pressure of 1×10^{-8} mbar onto the sample, CO was able to intercalate the water intercalated graphene islands. Often it was found that CO intercalation started from the gap formed where graphene island were crossing over Ir step edges. When more CO (100L – 300L) was dosed at low pressure (1×10^{-5} mbar), graphene islands were either completely intercalated or not at all. Furthermore, CO intercalated graphene was raised by 250pm from Ir(111) surface as well as the edges of fully CO intercalated graphene appeared smeared as if there were free dangling bonds on the edges. This indicates that may be CO intercalated graphene is detached from Ir(111) surface.

There is a formation of a 2-D confined environment between graphene and Ir(111) substrate and we can control what goes under graphene not only by the external parameters but also by modifying the graphene edges by intercalating graphene with something else first.

Outlook

The primary objective of this project was to study water assisted CO intercalation underneath Ir(111) supported graphene using STM. However, it is unclear whether the gap formed by the elevation of graphene due to water is responsible for CO intercalation or water modifies the graphene edges that enable CO intercalation or there is chemistry between water and CO that allows CO intercalation. To investigate this following experiments are proposed:

Intercalate graphene with inert molecules (e.g. Xe and Ar) so that they elevate the graphene islands and then dose high amount (≥ 1000L) of CO. If the graphene islands are intercalated by CO that means the elevation of graphene facilitates CO intercalation. On the other hand if there is no CO intercalation it implies that elevation of graphene is not the primary factor affecting CO intercalation. We did this and as seen from the figure below it was concluded that there was no CO intercalation.

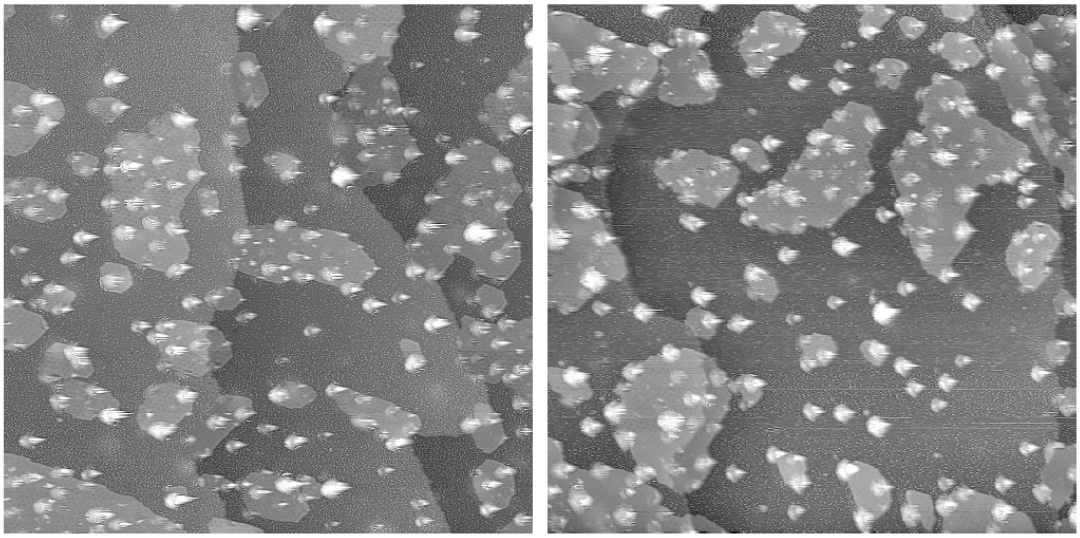

(a) (b)

Figure 31: (a) STM topography (100 × 100 nm) of Xe intercalated graphene on Ir(111) surface. (b) STM topography (100 × 100 nm) of Xe intercalated graphene on Ir(111) surface after dosing 1000L of CO.

Intercalate graphene with water by dosing low amount (1L - 5L) of O_2 and H_2. Than dose high amount (≥ 1000L) of CO and check the coverage of CO intercalated graphene. If all the graphene islands are intercalated by CO that means water modifies the edges of graphene that enables CO intercalation. On the other hand only some graphene islands are CO intercalated than it is the elevation of graphene due to water that facilitates CO intercalation.

One can also repeat this experiment with different molecule of same size and structure as CO and if all graphene islands are intercalated it implies that edge modification of graphene is responsible for intercalation. On the other hand if no intercalation is found one may conclude that it is chemistry between water and CO that enables intercalation.

From the results of above experiments, a firm conclusion could be made whether the gap formed by elevating graphene is responsible for CO intercalation or water modifies the graphene edges that enable CO intercalation or there is chemistry between CO and water that enable CO intercalation.

In general one can also try to form product of molecules in the 2-D confined environment created between graphene and Ir(111) substrate. For example first intercalate graphene with Xe and subsequently intercalate oxygen or fluorine and check if there is formation of XeO_4or XeF_2.

Bibliography

[1] P. Avouris, Nano Letters 10, 4258 (2010).

[2] R. Lv and M. Terrones, Materials Letters 78, 209 (2012).

[3] E. Roduner, Chemical Society Reviews 35, 583 (2006).

[4] A. Stierle and A. M. Molenbroek, MRS Bulletin 32, 1001 (2007).

[5] H. W. Kroto, J. R. Heath, S. C. O'Brien, R. F. Curl, and R. E. Smalley, Nature 318, 162 (1985).

[6] Grånäs E. Above and Below Graphene: Nanoparticle Chemistry and Interface Reactions. (2014).

[7] A. K. Geim and K. S. Novoselov, Nature Materials 6, 183 (2007).

[8] C. Nordling and J. Osterman, Physics Handbook for Science and Engineering, 6th ed. (Studentlitteratur, Lund, 2002).

[9] C. Lee, X. Wei, J. W. Kysar, and J. Hone, Science 321, 385 (2008).

[10] A. Kuzmenko, E. van Heumen, F. Carbone, and D. van der Marel, Physical Review Letters 100, 117401 (2008).

[11] F. Schedin, A. K. Geim, S. V. Morozov, E. W. Hill, P. Blake, M. I. Katsnelson, and K. S. Novoselov, Nature Materials 6, 652 (2007).

[12] C. Riedl, C. Coletti, T. Iwasaki, A. A. Zakharov, U. Starke, Physical Review Letters, 103, 246804 (2009).

[13] J. Robinson, M. Hollander, M. LaBella, K. A. Trumbull, R. Cavalero, D. W. Synder, Nano Letters , 11, 3875 (2001).

[14] P. Sutter, J. T. Sadowski, E. A. Sutter, , Journal of the American Chemical Society, 132, 8175 (2010).

[15] E. Starodub, N. C. Bartelt, K. F. McCarty, Journal of Physical Chemistry C , 114, 5134 (2010).

[16] M. Alif Arman Intercalation of CO and O2 under Ir(111) supported graphene: Studied by Scanning Tunneling Microscopy and X-ray Photoemission Spectroscopy. 2012.

[17] M. C. Weisskopf, B. Brinkman, C. Canizares, G. Garmire, S. Murray, and L. P. V. Speybroeck, Publications of the Astronomical Society of the Pacific 114, 1 (2002).

[18] M. Batzill, Surface Science Reports 67, 83 (2012).

[19] J. Wintterlin and M.-L. Bocquet, Surface Science 603, 1841 (2009).

[20] J. Coraux, A. T. N'Diaye, C. Busse, and T. Michely, Nano Letters 8, 565(2008).

[21] A. T. N'Diaye, S. Bleikamp, P. J. Feibelman, and T. Michely, Physical Review Letters 97, 215501 (2006).

[22] S. K. Hämäläinen, M. P. Boneschanscher, P. H. Jacobse, I. Swart, K. Pussi, W. Moritz, J. Lahtinen, P. Liljeroth, and J. Sainio, Physical Review B 88,201406 (2013)

[23] A. T. N'Diaye, R. van Gastel, A. J. Martnez-Galera, J. Coraux, H. Hattab, D. Wall, F.-J. M. zu Heringdorf, M. H. von Hoegen, B. Poelsema, C. Busse, and T. Michely, New Journal of Physics 11, 113056 (2009)

[24] P. Lacovig, M Pozzo, D. Alfé, P. Vilmercati, A. Baraldi, and S. Lizzit, Physical Review Letters 103, 166101 (2009)

[25] B. E. Nieuwenhuys, D. I. Hagen, G. Rovida, and G. A. Somorjai, Surface Science 59, 155 (1976).

[26] S. Lizzit and A. Baraldi, Catalysis Today 154, 68 (2010).

[27] J. Coraux, A. T. N'Diaye, M. Engler, C. Busse, D. Wall, N. Buckanie, F.-J. M.zuHeringdorf, R. van Gastel, B. Poelsema, and T. Michely, New Journal of Physics 11, 023006 (2009).

[28] H. Hattab, A. T. N'Diaye, Wall, G. Jnawali, J. Coraux, C. Busse, R. van Gastel,B. Poelsema, T. Michely, F.-J. M. zuHeringdorf, and M. H. von Hoegen, Applied Physics Letters 98, 141903 (2011).

[29] R. van Gastel, A. N'Diaye, D. Wall, J. Coraux, C. Busse, F.-J. M. zuHeringdorf,N. Buckanie, M. H. von Hoegen, T. Michely, and B. Poelsema, Applied Physics Letters 95, 121901 (2009).

[30] E. Loginova, S. Nie, K. Th□urmer, N. C. Bartelt, and K. F. McCarty, Physical Review B 80, 085430 (2009).

[31] E. Loginova, N. C. Bartelt, P. J. Feibelman, and K. F. McCarty, New Journal of Physics 11, 063046 (2009).

[32] G. Binnig and H. Rohrer, Surface Science 126, 236 (1983).

[33] G. Attard and C. Barnes, Surfaces, Oxford Chemistry Primers, 1 ed. (Oxford University Press, New York, 2009).

[34] B. Voigtlander, Scanning Probe Microscopy: Atomic Force Microscopy and Scanning Tunneling Microscopy, Springer

[34] Oura K. et al. Surface Science: An Introduction, Springer, (2010)

[36] Benjamin Hagman, Structure and reactivity of surface oxides on Cu(100), (2016)

[37] E.Grånäs, J. Knudsen, U. A. Schröder, T. Gerber, C. Busse, M. A. Arman, K. Schulte, J. N. Andersen and T. Michely ACS Nano 6 , 9951 (2012)